Development of a Generic Time-to-Contact Pilot Guidance Model

Linghai Lu[1], Michael Jump[2] and Gareth D. Padfield[3]
[1]*Faculty of Engineering and Technology, Liverpool John Moores University, Liverpool, L3 3AF*
[2,3]*Department of Mechanical, Materials and Aerospace Engineering, University of Liverpool, Liverpool, UK, L69 3BX*

Time-to-Contact (Tau, τ) theory posits that purposeful actions can be conducted by coupling the actor's motion onto the so-called τ-guides generated internally by their central nervous system. While the authors have made significant advances in the application of τ for flight control purposes, little research has been conducted to investigate how pilots are able to adapt their τ-guidance strategy to different aircraft dynamics; or how a τ-guide based pilot-aircraft model might be used to represent control behavior. This paper reports on the development of such a model to characterize the adaptation of pilot guidance to variations in aircraft dynamics using data obtained from a clinical pilot-in-the-loop flight simulation experiment. The results indicate that pilots tend to maintain a constant coupling between the dynamic system's motion and the τguide across a range of different configuration parameters. Simultaneously, the pilot modulates the guidance maneuver period to adapt to these different aircraft dynamics that result in changes in workload. Modelling the complete pilot stabilization and guidance function as a regulator plus inverter yields good comparative results between the pilot-aircraft model and simulator trajectory data and supports the hypothesis that the following of τ-based guidance strategies suppresses an aircraft's natural dynamics.

Nomenclature

a_g	=	acceleration due to gravity, ft/s^2
C	=	constant value

[1] Corresponding author, Senior Lecturer, l.lu@ljmu.ac.uk; Member AIAA.
[2] Senior Lecturer, mjump1@liverpool.ac.uk, Member AIAA.
[3] Emeritus Professor of Aerospace Engineering, gareth.padfield@liv.ac.uk.

G_{nm} = neuromuscular action system

k = coupling constant between motion and guide

K_L, K_P = regulating parameters

n_w = white noise in visual cue model

s = Laplace operator

t = time variable, sec

T = maneuver time that first reaches the center of target for the first time, sec

T_1 = maneuver time that finally stops at the center of circle, sec

v = rate of intrinsic gap closure, ft/s; pixel/s

$V(x, y)$ = inertial velocity in the x, and y axis, ft/s

x = distance to go in the x direction, ft, pixel

$\dot{x}, \ddot{x}$ = velocity and acceleration in the x direction, ft/s, ft/s^2 or pixel/s, pixel/s^2

$X(s)$ = Laplace transform of Δx

y = distance to go in the y direction, ft; pixel

$Y_c(s)$ = control element

$\Gamma(s)$ = Laplace transform of $\Delta\tau$

δ_{1c} = lateral cyclic stick input, inch

ζ = damping ratio

σ_{vis} = variance of n_w

τ = optical tau, the instantaneous time to close on a goal or gap, sec

ω = natural frequency, rad/s

Subscript

0 = initial condition

g = intrinsic τ guidance

nm = neuromuscular

Dressing Symbol

^ = normalized terms

I. Introduction

THE three functions of flight management and control performed by a human pilot – stabilization, guidance, and navigation – are described in Refs. [1-3]. The navigation function is a relatively long period, cognitive activity whilst the stabilization and guidance functions shape the pilot control inputs in the shorter term. A pilot normally performs these latter two functions simultaneously when, for example, terrain-following or target tracking. The stabilization, or compensatory function refers to the pilot's continuous correctional effort to avoid deviating from the desired flight state. This can be considered to be a relatively high-frequency control activity [1]. The guidance function is concerned with the avoidance of obstacles and the ground, essentially a flightpath management activity, and pilot control inputs are generally made at a lower-frequency than for the stabilization function. Of these, compensatory stabilization has been the most extensively studied for modelling the pilot-vehicle system [4-7]. The various features of a closed-loop system model associated with stabilization are well established, either through the development of new control algorithms or the creation of pilot models. However, studies of pilot guidance as a closed-loop function, the focus of this paper, are less common. This function is usually (and implicitly) implemented as a feedforward controller, through techniques such as inverse simulation [8;9] and nonlinear model inversion with feedback control [10]. Neural networks have also been used [11]. However, none of these approaches are particularly pertinent to an understanding of the underlying human dynamics.

Tau (τ) theory, based upon the perception of the instantaneous time-to-contact from the available optic flow when approaching an object or surface, provides a plausible means to model a human's perception and action for guiding movement [1;3;12;13]. This theory is based on the premise that purposeful actions are accomplished by coupling the actor's motion with either externally or internally generated guidance sources – the so-called motion guides [12;14;15]. Motivated by its application to pilots' visual perception, τ theory has already been applied to flight control and handling qualities [1;16-19]. The rationale for this line of investigation is that the overall pilot's goal is to overlay or close the gap between the perceived optical flow field and the required flight trajectory. The pilot then works directly with the available optical variables to achieve prospective control of the aircraft's future trajectory. One of the first applications of τ-coupling to aircraft flight considered τ-guide control strategies during a helicopter deceleration maneuver close to the ground [16]. An investigation of terrain-hugging flight reinforced the τ-based nature of the prospective control behavior of helicopter pilots [1;17;20]. Similar results have been found when applying τ-guide analyses to the landing flare maneuver of fixed-wing aircraft [18;19] and to the adverse aircraft-pilot

coupling phenomenon in a roll-step lateral re-positioning maneuver, described as boundary-avoidance-tracking [21]. In Ref. [3] it was suggested that pilots' τ–based actions effectively suppress the natural aircraft dynamics and this important aspect will be investigated in the present paper.

These previous studies generally support the hypothesis that the pilot adopts a τ-based strategy during guidance tasks. However, there are several potential barriers to the acceptance of such a hypothesis. First, within the psychology community, while there are advocates for τ theory, there are also its detractors, mainly due to very limited information known about perceptual timing [22]. Second, the use of time-to-contact and the associated τ-guides result in a fundamentally non-linear system that, at face value, adds mathematical complexity to the development of a guidance system and its subsequent analysis. Third, the use of τ-guides to control vehicle motion does not appear to be useful for pursuit guidance because of their apparent open-loop control structure. Finally, it is still an open research question as to how pilots use time-to-contact whilst having to adapt to the different vehicle dynamics that they encounter. Previous work has assumed that the τ-guide is a learned response, a mental model, to closing the desired motion gap [3]. Its position at the perceptual level for flight control is still unclear, whether it be compensatory, pursuit, or precognitive [6].

Perhaps because of these issues, τ is rarely used directly as a feedback control variable in the literature. For example, the work in Ref. [23] studied pilot guidance strategy using an adaptive pilot model (APM) when performing the ADS-33 Acceleration-Deceleration maneuver. Reference [25] reported the development of a τ-following controller for automatic helicopter deck landings. However, despite notionally being studies into the use of τ, neither explicitly used τ within the control loops developed. Similarly, most studies in the unmanned aerial vehicle (UAV) and bio-inspired guidance literature, which should be ripe for τ-based control, are usually based upon the maintenance of a constant ventral optical flow, rather than the adoption of a τ-guide guidance strategy [26-28]. However, a small number of research activities have used τ to provide vehicle guidance solutions. Here, τ is either computed indirectly by measuring the motion gap and the gap closure rate [29] or by extracting the time to contact from the observed optical flow using feature scales [30].

Motivated by this apparent lack of adoption of τ as a useful guidance mechanism and control variable, this paper reports on a pilot-aircraft model developed to better understand how pilots might use τ guidance as a means of motion control that, in turn, allows some of the issues noted above to be addressed. The paper proceeds as follows. The key elements of τ theory pertinent to the paper are briefly reviewed in Section II. Section III describes the pilot-aircraft

model structure used and Section IV provides a description of the experimental set-up used to help understand how the system model should be configured. Section V reports on the results of the experimental test campaigns and then Section VI discusses further developments of the τ-guide model. The results of the experiments and the pilot-aircraft model analysis are discussed and concluded in Section VII and VIII, respectively.

II. Review of Motion Guidance Using τ Coupling

Tau theory is based upon the fundamental parameter, τ, the time-to-contact variable in the optical field [12],

$$\tau(x,t) = \frac{x}{\dot{x}} \tag{1}$$

where x is the perceived (negative) motion gap to be closed and $\dot{x}$ is the instantaneous gap closure rate, as illustrated in Fig. 1.

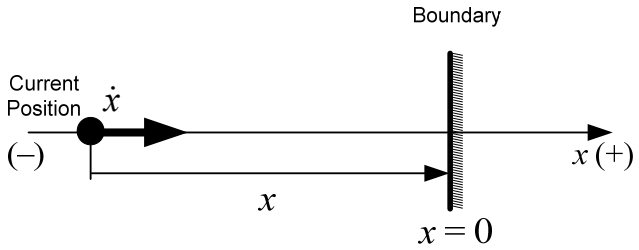

Fig. 1 Kinematics of closing a perceived motion gap

The τ concept was formulated by Lee [12] when modelling how animals prospectively control their movement through a cluttered environment. The 'motion-gap' concept can be extended to encompass other parameters that can be sensed, such as tactile forces (e.g., when taking a step or grasping a handle) or auditory signals (e.g., whilst playing an instrument or singing a song) [15]. Critically, τ is hypothesized to be directly perceived by observers i.e. without the need for intermediate cognitive reasoning, to control the gap closure efficiently. It is further hypothesized that this is the result of natural evolutionary processes – the guidance of movement should be simple, rapid, reliable, and biologically plausible. If this were not the case, the guidance process might be degraded by any associated delays and noise resulting from lengthy computations or cognitive thought processes [12;15]. Several examples offer evidence to support this hypothesis [12;14;15;17].

In practice, there is often more than a single gap that needs to be closed, such as the coordination required between the lateral and longitudinal motions when an animal closes on its prey or forward and vertical motions required to land an aircraft [18]. Two motions, $x(t)$ and $y(t)$, are said to be τ coupled if the following relationship is satisfied,

$$\tau_y = k\tau_x \tag{2}$$

The constant coupling term k in Eq. (2) regulates the dynamics of the motions in the x and y directions. By keeping the τ's of motion gaps in a constant ratio, it can be shown that this τ-coupling results in effective guidance through a power law (for $x < 0$, and $y < 0$) [12],

$$y = C \cdot (-x)^{1/k} \tag{3}$$

The negative sign in Eq. (3) is due to the convention in τ theory that defines motion gaps as closing from negative values to zero [12]. Therefore, the constant C must also be negative in order for y to be negative. Tau-coupling can take two forms; extrinsic (x and y are physically observable) or intrinsic (x is physically observable while y is generated by the actor's central nervous system). The second situation occurs when movements are self-guided and there is no second extrinsic motion gap to couple onto, such as when playing a piano. Here, there is a physical motion gap to close (between finger and key) but that gap closure must be coupled to the rhythm of the tune being played, which is internally generated [15]. Under these circumstances, the motion gap is hypothesized to be coupled onto a so-called 'intrinsic' motion guide. Intrinsic τ-guidance is modelled using the relationship,

$$\tau_x = k\tau_g \tag{4}$$

The intrinsic τ-guide, τ_g, defines a motion that is guiding a moving target with its own τ. It can take a number of different forms, but the most interesting and relevant for this paper is the Constant Acceleration Guide (CAG). This can be used to model Acceleration-Deceleration motions, e.g. guiding a rotorcraft from one hover position to another [1;15]. The detailed derivations of the motions for τ_g are given in Table A1 for completeness. In the Table, a_g is the acceleration of the τ-guide and v_{g0} is its initial speed. The dressing '^' indicates that the temporal variables are normalized by T, the duration of the maneuver, such that $0 < \hat{t} \leq 1$. Examples of the motions that can be generated by varying the values of the coupling constant, k, are shown in Fig. 2. Finally, the interpretation of the various values of k, can be found in Table A2. From these derivations, it can be observed that τ-coupled motion is only dependent upon the parameters k and T.

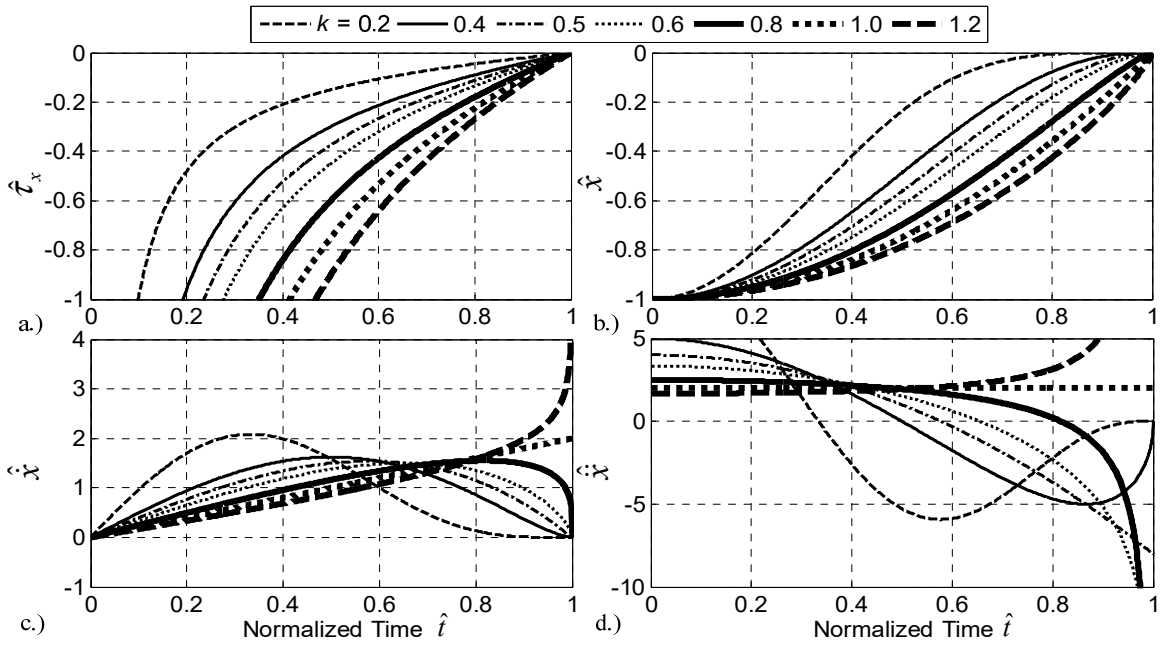

Fig. 2 Examples of motion τ, gap, gap closure rate, and gap closure acceleration when coupled with a constant acceleration τ-guide

III. Modelling of Pilot's Visual Guidance Strategy

A. Pilot-Aircraft Model Structure

To model the pilot's visual guidance strategy using an intrinsic τ-guide, an appropriate pilot-aircraft model structure must be established, characterizing the visual information available to the pilot that then flows through the controlled elements. This requires that the different behavioral features of the pilot model are characterized [6]. The classical types of pilot-vehicle system structure normally deal with the closed-loop control situation, where explicit external reference inputs are available. These are typically either compensatory, where the pilot closed-loop response is derived from certain errors (e.g., position or attitude), or pursuit, where the pilot follows a command input [7]. However, this kind of externally perceived error cue is not present for the present investigation, but rather it is postulated that the guidance signal is generated internally by the pilot based on the perceived visual cues. This is, of course, why the τ-guide of Eq. (4) appears to be open-loop. To address this issue, the pilot-vehicle closed-loop structure of Fig. 3 was used.

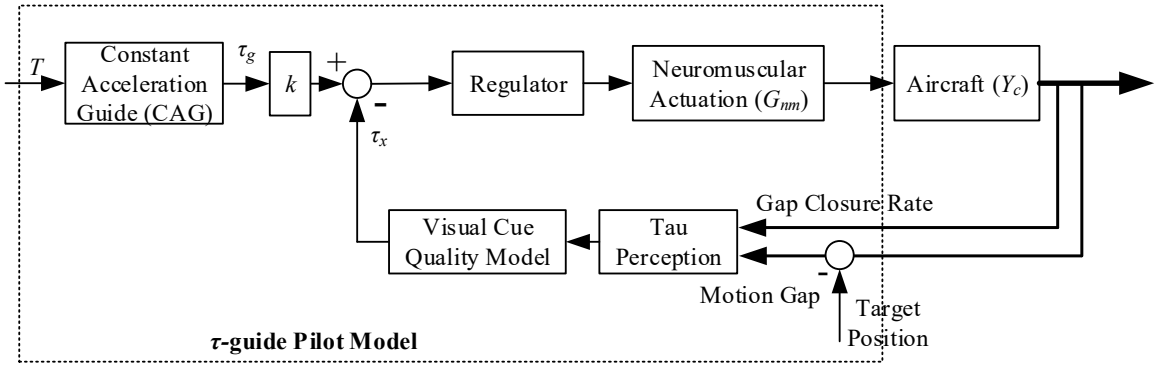

Fig. 3 Pilot model with constant acceleration guide

The model structure of Fig. 3 emphasizes the visual control channel, which generally reflects the experimental set up described in this paper, where the visual stimuli are dominant. The reasons for proposing this model structure are outlined briefly below.

First, a closed-loop error-correcting structure is assumed following the hypothesis that the pilot acts in response to the errors between the guidance command ($k\tau_g$) and the perceived τ_x. The proposed structure complies with the fundamental hypothesis of τ theory i.e. the overall pilot's visual guidance strategy is to overlay the perceived optical flow-field onto the required flight trajectory. The pilot then works directly with optical variables (τ) to achieve prospective control of the aircraft's future trajectory (τ_x), by selecting the appropriate k and T values; the pilot's selection will depend upon operational circumstances (e.g. need for agility) and the aircraft performance (e.g. thrust or power margin). The element of the pilot activity that achieves the desired tracking performance is modelled as a regulator driven by the error between the desired and perceived optical τ trajectories.

Second, the pilot model operates directly on the optical τ information sensed from the available optic flow, instead of positional or velocity information as in Ref. [25] or, for example, Hess's pursuit tracking pilot model [31]. This more appropriately reflects the hypothesis that τ information is perceived directly by the pilot, without the need for intermediate reasoning or computation. Thus, the main visual cue for the pilot model of Fig. 3 will be the τ variable sensed from the optical flow. As a result, the τ-guide pilot model of Fig. 3 can be differentiated from the τ-following feedback controller in, for example, Ref. [28].

B. Development of the Regulator

The first task associated with the application of the proposed model in Fig. 3 is to design an appropriate form of regulator. Two points need to be considered here. First, what kind of control strategies are being used in the timing of the information perception process – continuous or intermittent [12;22]? The guidance strategy, mainly developed by Lee [12], assumes that a continuous control input (after the regulator) is activated by the visual system through the continuous stimulation of the retina. In contrast, an intermittent process uses optical τ information to modulate control activity only at discrete moments during the maneuver [32]. This paper adopts the continuous-feedback-control model using optical τ information on the premise that, for the simple experiment scenario being explored, the pilot's control activity follows the information perception synchronously as there is only one visual task being undertaken.

The second point to be considered when designing the regulator stems from the nonlinearity originating in the τ function defined in Eq. (1). This nonlinearity can result in a difficulty in constructing a linear regulator to achieve the desired closed-loop system tracking performance. Also, the τ function is numerically unstable from a computational point of view in that a small (or even zero) velocity in the initial (or final) phase of the maneuver can make the fluctuation of τ values large (or infinite) [13]. The (linear) regulator was developed to address this problem by linearizing the nonlinear τ variations, as follows.

If, assuming a state (x_{b0}, $\dot{x}_{b0}$) within which x_{b0} is the instantaneous gap to the possible target during the maneuvering period in Fig. 1, Eq. (1) can be linearized using a Taylor series expansion as shown in the following,

$$\tau(x_b, \dot{x}_b) \approx \tau(x_{b0}, \dot{x}_{b0}) + \dot{x}_{b0}^{-1}(x_b - x_{b0}) - x_{b0}\dot{x}_{b0}^{-2}(\dot{x}_b - \dot{x}_{b0}) \tag{5}$$

in which the higher-order terms are assumed to be small levels of noise in the perception process and therefore are ignored in the formula. Simplification of Eq. (5) thus yields the general solution for the change in τ in terms of x,

$$\Delta\tau(x_b, \dot{x}_b) \approx \tau(x_b, \dot{x}_b) - \tau(x_{b0}, \dot{x}_{b0}) = \dot{x}_{b0}^{-1}\Delta x_b - x_{b0}\dot{x}_{b0}^{-2}\Delta\dot{x}_b \tag{6}$$

in which $\Delta x_b = x_b - x_{b0}$ and $\Delta\dot{x}_b = \dot{x}_b - \dot{x}_{b0}$. The Laplace transform of Eq. (6) can be written as follows,

$$\Gamma(s) = (\dot{x}_{b0}^{-1} - x_{b0}\dot{x}_{b0}^{-2}s)X(s) \tag{7}$$

in which $\Gamma(s)$ and $X(s)$ are the Laplace transform of $\Delta\tau$ and Δx_b, respectively. Three points to note relating to the above procedure are as follows. First, the instantaneous gap (x_{b0}) measuring the current distance to the target and the optical variable τ, by definition, are negative. However, the increments of both $\Delta\tau$ and Δx_b are positive with a positive speed

of approach to the target ($\dot{x}_{b0}$). Second, the forms given in Eqs. (6) and (7) that rely on $\Delta\tau$ information are consistent with the findings of the recent study of information used to detect upcoming collisions by Bootsma and Craig [32]. They found that the information carried in $\Delta\tau$ is the most effective predictor for collision avoidance. Finally, the perception of the optical τ information is modelled in Eq. (7) as a lead equalization by the pilot, given by the following:

$$\Gamma(s) = (T_{b0}s + 1)K_{b0}X(s) \tag{8}$$

in which $T_{b0} = -x_{b0}\dot{x}_{b0}^{-1}$, the initial τ to the target and $K_{b0} = \dot{x}_{b0}^{-1}$. Considering this lead function in the closing of a gap, the following structure was proposed for the regulator:

$$C(s) = \frac{K_P}{s}(s + K_L) \tag{9}$$

in which K_P and K_L are the pilot gain and lead-equalization values, respectively. The gain term K_P is used to achieve the desired tracking performance. The integrator was included to ensure zero steady-state error, even in the presence of controlled element variations [33]. The term ($s + K_L$) was introduced to represent the lead equalization in Eq. (8) from the optical τ-perception process as described above.

C. Modelling the Remaining Elements of the Pilot Model

The neuromuscular action system (G_{nm}) of the pilot in Fig. 3 was modelled as a second-order transfer function as follows [31;34],

$$G_{nm} = \frac{\omega_{nm}^2}{s^2 + 2\zeta_{nm}\omega_{nm}s + \omega_{nm}^2} \tag{10}$$

in which ζ_{nm} is the neuromuscular damping ratio and ω_{nm} is the corresponding natural frequency. The generic values, 0.30 and 9 (rad/s), from Ref. [35] were chosen for these two parameters (ζ_{nm} and ω_{nm}), respectively. The visual model of Eq. (11) was adopted to reflect the quality of visual information sensed by the pilot in Fig. 3 [34],

$$(1 + n_w) \cdot \frac{1}{0.5s + 1} \tag{11}$$

in which n_w is a zero-mean, normally distributed random variable with variance σ_{vis} that is equivalent to the noise–signal ratio of injected observation noise in algorithmic pilot models [36]. Eq. (11) indicates that the sensed visual cue is first contaminated by an external noise original n_w and then passes thought a low-pass filter. The better the visual cues, or the useable cue environment [24], the lower is the value of σ_{vis} (σ_{vis}= 0 means no visual cue degradation). For

the results presented in this paper, the σ_{vis} value was selected to be 0.02, to represent the good visual environment used for the experiment performed in the simulator for the study reported later [34].

IV. Experimental Set-Up

To establish the parameters of the τ-guide required for the pilot model, a 'clinical' investigation into single–axis control of an element, where the dynamics of the controlled system are defined precisely, is described in this Section.

The aim of this experiment was to investigate the adaptation of a pilot's guidance strategy using the pilot-aircraft model of Fig. 3, when the parameters of the controlled system are varied [3]. There were two requirements for this experiment. First, the selected task should be representative of a simple flight maneuver. Second, the investigation should span a wide range of dynamic properties for manned aircraft types, to make the conclusions generally meaningful. To meet these requirements, the following experimental configuration was developed.

The experiment was conducted using the University of Liverpool's (UoL's) HELIFLIGHT simulator [37] shown in Fig. 4.

Fig. 4 External and internal views of HELIFLIGHT research simulator at the UoL ([38])

A display was developed for HELIFLIGHT's outside-world-center visual channel that contained a circular 'ball' and circular 'target'. This is illustrated schematically in Fig. 5. The pilot's task was to move the ball from rest at its initial left-hand position (A) and bring it to rest at the final right-hand position (B), inside the target using the lateral cyclic stick. This is akin to a highly simplified lateral-reposition task of the ADS-33 [24].

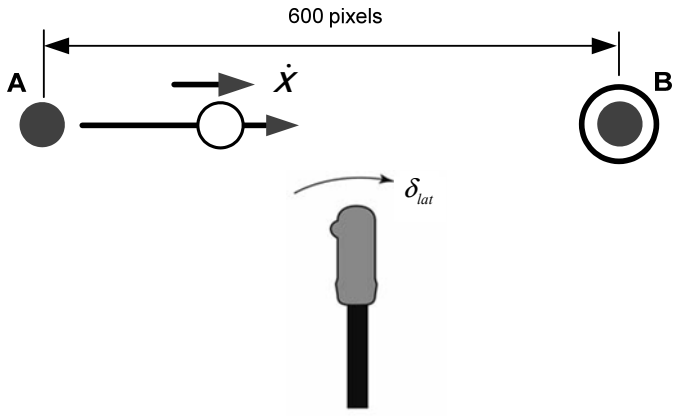

Fig. 5 Schematic of single-axis lateral-reposition pilot task [3]

The dynamics between the lateral stick input (δ_{lat}) and the ball were modelled as a second-order system that characterizes a typical aircraft equivalent low-order system [1]:

$$\frac{X}{\delta_{lat}}(s) = \frac{5.2\omega_n^2}{s^2 + 2\zeta\omega_n s + \omega_n^2} \tag{12}$$

in which ω_n is the natural frequency, ζ is the damping ratio, and $X(s)$ is the Laplace transform of the motion gap x. The gain of 5.2 represents the scaling factor between stick (in inches) and visual gap (in pixels). For the system illustrated in Fig. 5, position A was the origin and position B was the target end position for the ball symbol, 600 pixels to the right. The motion gap, x, was then defined to be the negative distance from the current position to point B in pixels.

The natural frequency (ω_n) and damping ratio (ζ) have a significant influence on the 'handling' characteristics of a system [24]. How the dynamic properties might impact a pilot's impression of the vehicle's response is summarized in Fig. 6 [3].

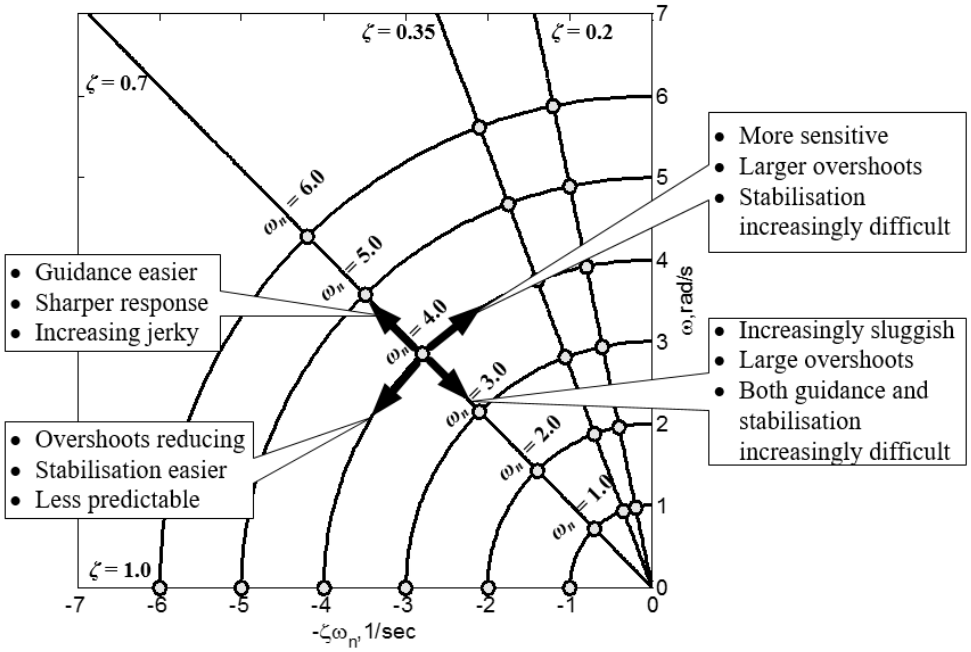

Fig. 6 Typical Pilot Opinions of the Handling Qualities in A Maneuvering Task with Simple Second-Order Dynamics [3]

The configuration of the controlled system was changed by adjusting ω_n and ζ. Twenty-four different configurations, represented by the circular dots shown in Fig. 6, were chosen for investigation. These were considered to be representative of the dynamic properties of a range of stable aircraft [3]. The parameter under investigation for each test point was always varied from the baseline or reference configuration defined by $\omega_n = 4,\ \zeta = 0.7$. This is the region in Fig. 6 where it is considered that pilots are able to achieve good performance with low 'workload' for tracking tasks [39]. This procedure was used to try to ensure consistent pilot performance for the different configurations. For example, having completed the test with a new (non-reference) configuration, the subjects were required to 're-fly' the test using the reference configuration before commencing the next test with a new set of non-reference parameters.

Four subjects participated in the experiment: a rotary-wing test pilot (RWTP), a rotary-wing pilot (RWP) and two fixed-wing pilots (FWP1 and FWP2). The RWTP was only able to participate in 14 of the available dynamics configurations. Subjects were instructed to conduct the task promptly but whilst taking sufficient time to achieve the task of arresting the ball within the outer ring in Fig. 5, without overshoot. To be clear, this meant that during the conduct of each test, the subject could freely select the overall maneuver period of the task. The task was considered

to be complete after pilots had maintained the ball within the target circle for 3 seconds. This is consistent with the input used for the pilot model in Fig. 3.

V. Experimental Results

A. Variable Dynamics Test Campaign Results

The test required the subjects to close only one motion gap. The ball started at rest, was accelerated to some translational velocity and was then decelerated back to rest again within the target zone by using the lateral cyclic stick. The Acceleration-Deceleration motion profile is typical of motion generated by coupling the guided motion onto the intrinsic CAG discussed in Section II. Assuming the relationships of Eq. (4) and the motion profiles of Fig. 2 and Table A1, the values of k and T required to generate such a coupled motion can thus be computed from the time histories. In this case, the time T is defined as the time taken for the ball to be moved from position A to the first time that it reached position B. The results obtained for each of the various dynamic configurations tested are shown in Fig. 7 and Fig. 8.

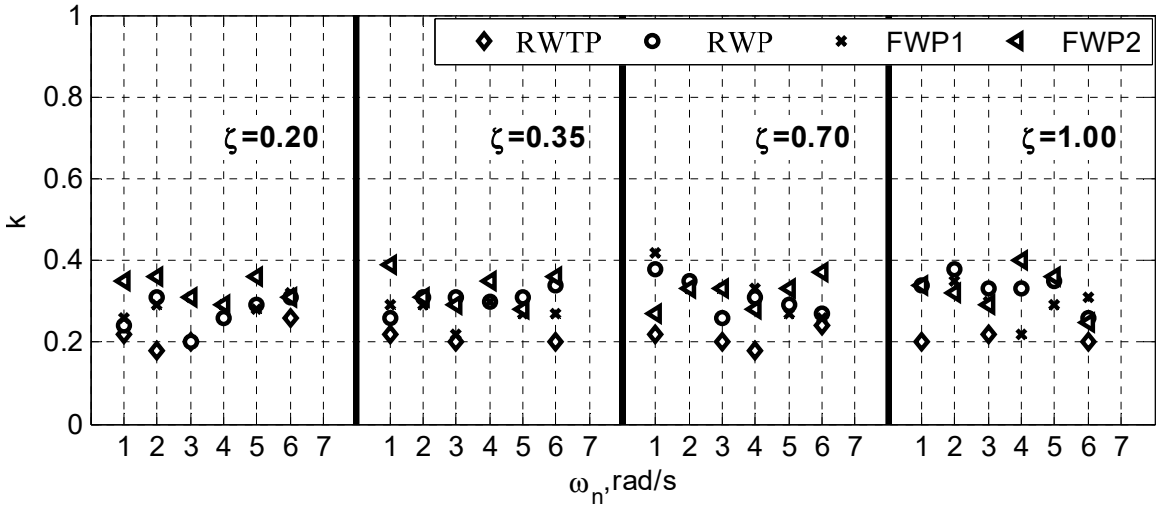

Fig. 7 Variation in coupling parameter *k* with system parameters

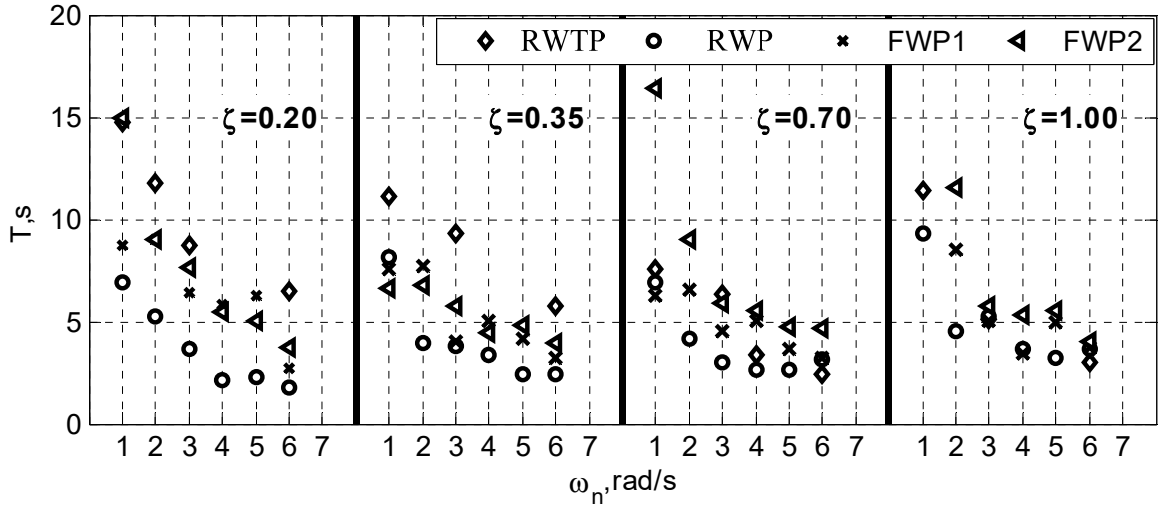

Fig. 8 Variation in maneuver time *T* with system parameters

The distribution of the k values from all four subjects (with mean value $\approx$ 0.28) indicates a relative insensitivity of the pilot's guidance strategy to the frequency and damping ratios of the controlled element (the ball). Moreover, the range of values of k between 0.2-0.4 means that the maximum velocity for the maneuver consistently occurred in its 2nd quartile i.e. all of the test subjects initiated the deceleration of the ball in the second quarter of the maneuver, before the half way point of the gap was reached (item 5 in Table A2).

In contrast, the maneuver times (T) reduce as the natural frequency increases. Fig. 8 shows that pilots elect to slow the maneuver down as ω_n decreases to deal with the deteriorating natural dynamics of the system (akin to vehicle handling qualities degrading). The inverse relationship between T and ω_n suggested by the data in Fig. 8 reinforces the idea of an upper limit to achievable 'task frequency' for a given system frequency (Ref. [1], section 5.2.2). Moreover, the decreasing trend in T seems to be reasonably independent of the damping ratio used. The results show that the natural frequency of the controlled system has a more dominant influence on the adaptation of the controller's guidance strategy than the damping ratio for this task. As would be expected, with faster dynamics (i.e. a larger ω_n value), the subjects tend to accomplish the task in a shorter time.

B. Ideal Control Inputs for the Intrinsic τ-Guide

Tau theory posits that the control of movement uses the directly perceived motion information available from the optic flow [1]. Traditionally, this information flow process is described by the identification of the coupling terms (e.g., k and T values as investigated above) from the optical states. Therefore, with the estimated k and T values and

the known intrinsic guidance strategy, the 'ideal' control activity may be determined inversely from the postulated intrinsic guidance signals for comparison with the measured control activity.

The pilot control command (δ_{latg}) required to perform this guidance maneuver can be predicted using Eq. (13).

$$\delta_{latg} = \frac{1}{5.2}\left(\frac{1}{\omega_n^2}\ddot{x} + \frac{2\zeta}{\omega_n}\dot{x} + x\right) \tag{13}$$

As far as the intrinsic CAG is concerned, the normalized motion gap, velocity, and acceleration required in Eq. (13) are determined from Table A1 and are the same for all dynamic configurations.

The approach used to calculate δ_{latg} is similar to the inverse-simulation methodology used to derive the required inputs for a given flight trajectory [9]. Importantly, the calculated 'ideal' input is not contaminated by any stabilizing control activity and, in fact, the natural dynamics (the poles of Eq. (12) of the aircraft model that become zeros in Eq. (13)) are not the dominant factors for determining the response characteristics of the required δ_{latg}. The dynamics of the closed-loop motion are mainly determined by the zeros, not the original poles characterized by the ω_n and ζ values in Fig. 6 [33;40]. Moreover, the linear 2nd-order system used in this paper is a minimum-phase system and has no zeros. Therefore, the inverted inputs are stable and their dynamics are uniquely determined by the ideal trajectory information provided (τ_x). The dynamics of the model are totally suppressed using these 'ideal' inputs, which of course vary as the natural frequency and relative damping vary. The results of three representative configurations flown by Pilot RWTP are compared with the ideal pilot inputs in Fig. 9.

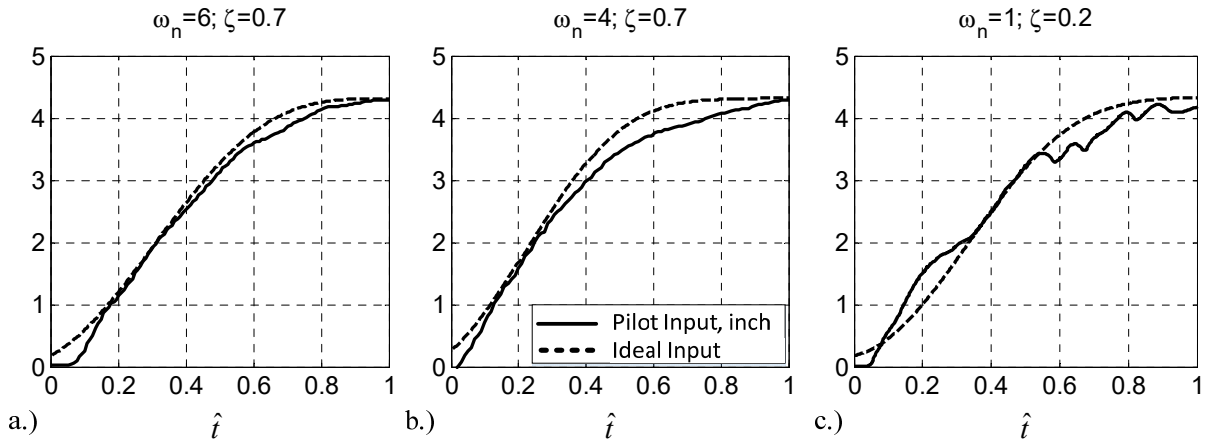

Fig. 9 **Comparison between the ideal and actual pilot inputs (Pilot RWTP)**

Case Fig. 9 (*a*) represents a case from the region of Fig. 6 that predicts good tracking performance, Case Fig. 9 (*b*) is the baseline configuration, and Case Fig. 9 (*c*) has dynamics where a poorer tracking performance would be

expected. An Input Fitting Index (IFI) is proposed here to measure the fit between the ideal and actual pilot inputs. The lower the value of the index, the better the agreement between the two data sets.

$$Input\ Fitting\ Index = \frac{\int_0^T \left|\delta_{latg} - \delta_{lat}\right| dt}{\int_0^T \left|\delta_{latg}\right| dt} \cdot 100\% \tag{14}$$

The fit is computed through the integration of the difference between the actual pilot input and the ideal intrinsic τ-guided input. The IFI values from the experiments for all four pilots are shown in Fig. 10.

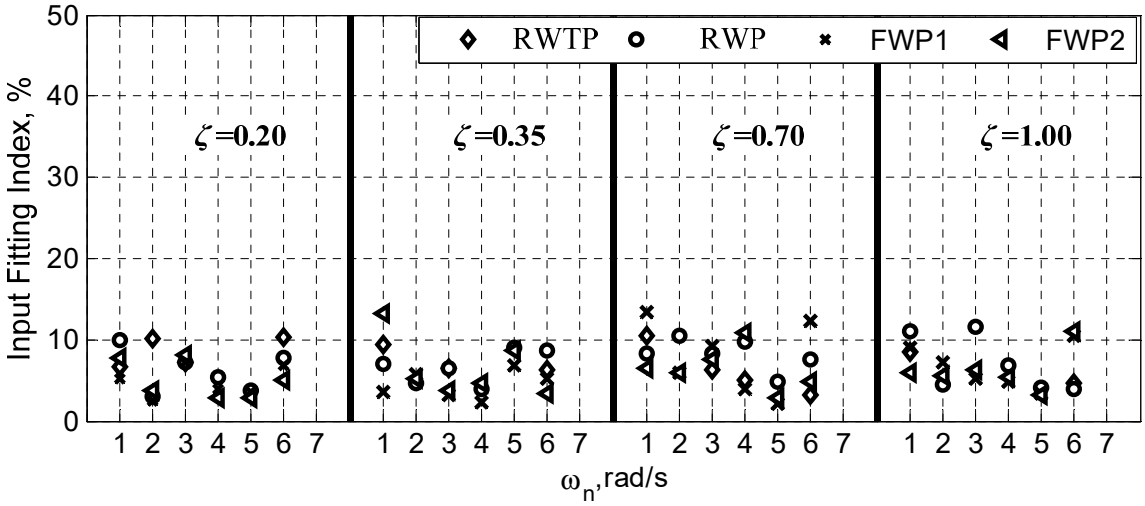

Fig. 10 Fit index for pilot control inputs and ideal τ-guided inputs

The comparisons in Fig. 9 show that the pilot inputs generally match the ideal inputs used to move the ball from position A to B. These results support the hypothesis that the pilot response can be modelled assuming that the CAG is being followed during this task. The ideal control inputs are different for the different cases of course, but a common feature is that the natural dynamics are suppressed by τ-following control strategies. However, the actual pilot input for cases like e.g. $\omega_n = 1,\ \zeta = 0.2$ in Fig. 9*c*, are 'contaminated' with minor oscillations due to the lower natural frequency and damping ratios that lead to increased pilot 'stabilization' activity being required. With no external disturbance, the stabilization is the corrective action to errors in the τ guidance that excite the system's natural dynamics as illustrated in the model structure of Fig. 3. This higher-frequency control activity is absent from the model prediction in Eq. (13). The reason for this is given above i.e. the inversion process in Eq. (13) nullifies the natural dynamics of the system.

The difference between actual and ideal control inputs shown in Fig. 10 is less than 15% across the different frequency and damping configurations tested. These findings are consistent with all the results obtained from the other three pilots used in the tests, which, for the sake of brevity, have been omitted from the paper.

C. Workload Estimation

The ideal pilot input (δ_{latg}) derived using Eq. (13) represents only the guidance function of a pilot's control activity. The difference between the actual and ideal pilot inputs shown in Fig. 10 is the test subject's compensation for errors in judgement (guidance), which takes the form of additional high-frequency stabilization control activity required across the varying aircraft dynamics. However, the part of maneuver used in Eq. (13) only includes the period of moving ball from Position A to first reaching the center of Position B. As mentioned in Section IV, the test subjects were also required to stabilize the motion of the ball and to bring it to rest within the target circle (position B). This stabilization control activity contributes to, and can even dominate, the total pilot compensatory control effort as the ball approaches the desired rest position. This usually requires finer and more precise control inputs than for the initial guidance phase of the motion. Therefore, the results in Eq. (13) are incomplete in representing the total pilot's compensatory activity during the experimental testing.

In addition, the results in Fig. 8 indicate the reasonably high sensitivity of the maneuver times (T) to ω_n, ranging from the shortest of 2 sec to the longest of 15 sec. The pilots appear to have dealt with the low ω_n configurations by adopting a strategy of increasing the maneuver period. This can, in turn, increase the mental and temporal demands of the task. It may be that these demands can be understood by considering the maneuver time for the different dynamic configurations investigated in the paper. The time-weighted Total Compensatory Effort (TWTCE) is widely used in the control field to measure the performance of a system [41]. It is therefore proposed here as a means to account for the influence of the maneuver time on the pilot control activity, split between stabilization and guidance activity. In some sense, this might therefore be considered as a measure of pilot workload.

$$TWTCE = \frac{1}{T}\frac{\int_0^T t\left|\delta_{latg} - \delta_{lat}\right| dt}{\int_0^T \left|\delta_{latg}\right| dt}\cdot 100\% + \frac{1}{(T_1 - T)\delta_{latg}(T)}\int_T^{T_1} (t - T)\left|\delta_{lat}(t - T) - \delta_{latg}(t - T)\right| dt \cdot 100\% \tag{15}$$

where T_1 is the complete period during which the ball is being brought to rest at the center of the circle (position B). Equation (15) physically describes the percentage of the deviation of the timed-weighted actual control input from the timed-weighted ideal control input. The latter is defined as the ideal control effort required in Eq. (14) to achieve the

lateral-reposition task without it being 'contaminated' by any stabilization activity. The results calculated from the experiment for the four test subjects using Eq. (15) are shown in Fig. 11.

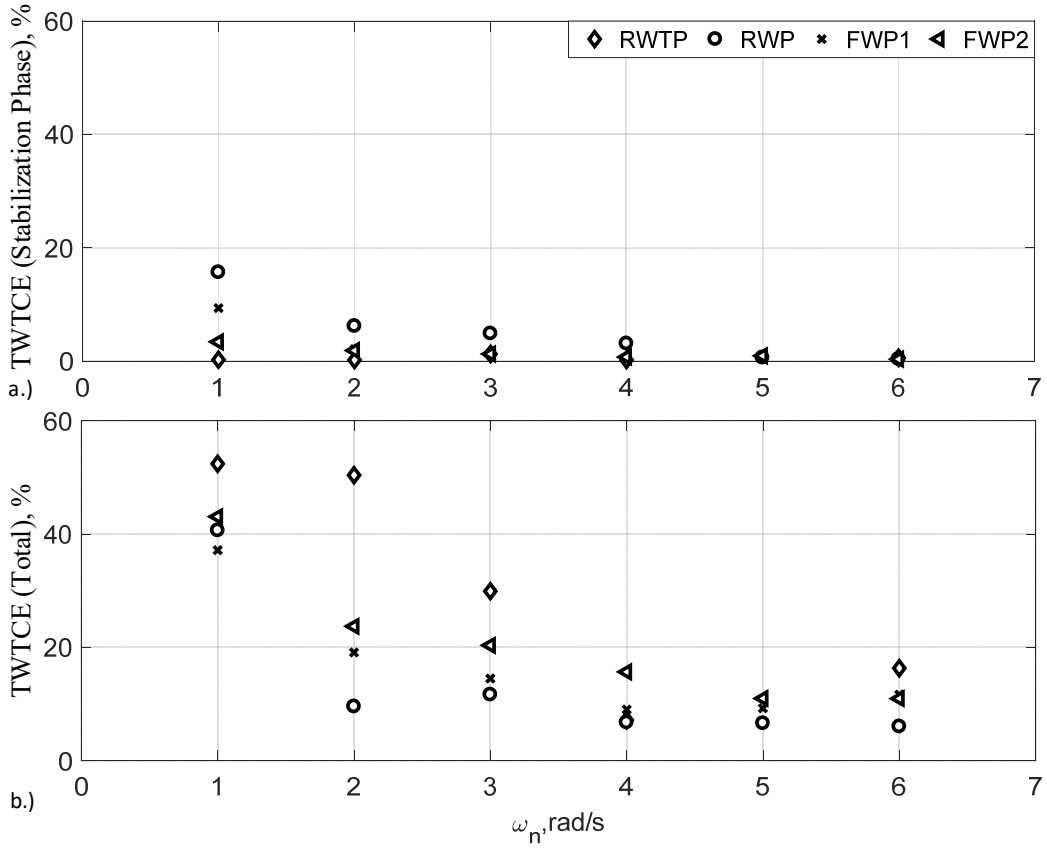

Fig. 11 Total mean time-weighted compensatory effort for the whole lateral-reposition maneuver

Fig. 11(*a*) represents the additional compensatory effort required after first reaching Position B and Fig. 11(*b*) represents the total compensatory effort from the beginning to the end (with the ball at rest at the center of the circle at Position B) of the maneuver. Each data point in Fig. 11(*a*, *b*) is the averaged TWTCE value for each dynamic configuration having the same ω_n value but for all ζ. This has been done to strengthen the distribution characteristics of the pilot workload variation across ω_n. The distribution in Fig. 11(*a*, *b*) is consistent with that of Fig. 6, showing the increasing difficulty in both guidance and stabilization for these configurations. There is an apparent small increase in workload for ω_n = 6 rad/s. This may be due to the pilots' need to apply additional control effort to overcome the sharper response of the system as the bandwidth of the system increases.

VI. Configuration and Validation of the Pilot-Aircraft Model

The results of Sections III and IV can be used to configure the postulated pilot model. Section V provides data against which the model can be compared. However, the regulator values, K_P and K_L, in Fig. 3, are not yet known. Once these were computed, the effectiveness of the model structure could be assessed. Assuming the modelling to be successful, it can then be used to aid understanding of the issues raised earlier in the paper, such as the difference between the ideal and actual pilot inputs shown in Fig. 9, and the apparent suppression of the vehicle dynamics, resulting in the motion response being dependent only on the maneuver period, T, and the coupling constant, k.

A. Determination of Regulator Parameters

The regulator gain values, K_P and K_L, in Fig. 3, were found by minimizing the squared feedback error of the two sets of tracking signals applied at the summing junction for τ_x in Fig. 3 ($\tau_x - k\tau_g$): the ideal τ signals (annotated as 'Ideal τ' in the following) with k and T values in Fig. 8 and the τ signals based on the actual pilot activity (annotated as 'Piloted τ' in the following) using Eq. (1). Comparisons of the K_P and K_L values obtained from these two sets of tracking signals should reveal the differences in actual and ideal pilot activities shown in Fig. 9 and in Fig. 10. The values obtained for the 14 test configurations of the controlled elements conducted by Pilot RWTP are illustrated in Fig. 12.

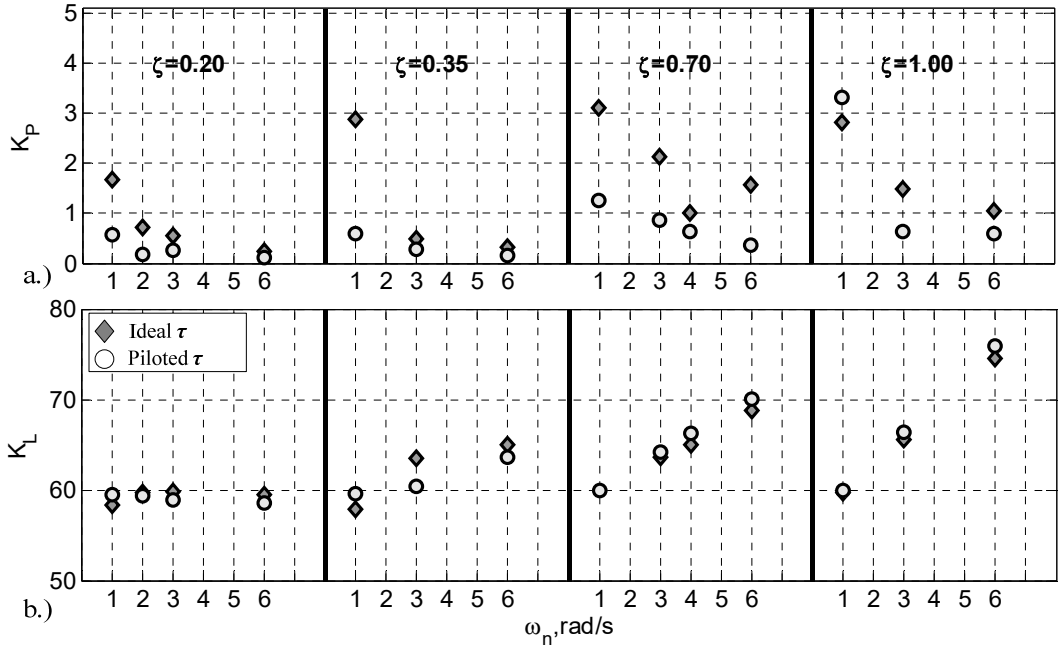

Fig. 12 K_P and K_L values for 14 configurations of controlled elements (RWTP)

The results of Fig. 12*a* show that the two sets of K_P values have a generally similar trend but deviate somewhat in magnitude for the configurations with the slowest motion (minimum ω_n). This distribution resembles that of the estimated maneuver time (T) in Fig. 8. This may indicate that the pilot tends to adopt larger gains and take a longer time to achieve the slower-motion configurations. This is consistent with the larger time-weighted workload shown in Fig. 11 and with Eq. (13) in that larger inputs are required for smaller ω_n to achieve the same response. Larger control inputs are to be expected as the response becomes more 'sluggish' [1].

The pilot lead term in Fig. 12*b*, K_L, is the inverse of a time constant in Eq. (9) and hence is an equivalent quantity to a frequency. This high-frequency term models the rapid perception, with the lead-equalization characteristic based on the linearized analysis in Eq. (8). Its values vary within the range 50 – 75 rad/s (see Fig. 12*b*). These are generally consistent with a human's visual reaction bandwidth, estimated to be 30 – 70 rad/s, depending on the type of task attempted [13]. Moreover, Fig. 12*b* shows that K_L becomes larger as the damping, ζ, increases. This is physically reasonable; as the system become less predictable (Fig. 6), the pilot needs to make improved anticipatory inputs to maintain the desired control performance.

B. Effectiveness of the Proposed Pilot-Aircraft Model

The effectiveness of the pilot-aircraft model in Fig. 3 was examined by driving the pilot-aircraft model, individually, using two τ commands: the Ideal τ using k and T values from Fig. 7 and Fig. 8, and the Piloted τ. These τ commands were applied at the summing junction for τ_x in Fig. 3, using the gain values of Fig. 12. The control inputs (after G_{nm} in Fig. 3) from these offline simulation processes, as well as the aircraft model outputs were then compared.

The comparisons presented below uses data from Pilot RWTP (for 14 dynamic configurations). During the offline simulations, the τ-perception feedback loop of Fig. 3 is only activated when the closure velocity ($\dot{x}$) is larger than 0.01 pixel/s (the average maneuver speed is around 200 pixel/s), to avoid the singularity in Eq. (1) when $\dot{x} = 0$. The adjustment of this activation timing should have little effect on the results, the pilots commenting that they adopted an open-loop control strategy for a short period in the initial phase of the maneuver; arguably before any τ-guidance was activated.

Typical results from the offline simulation for three configurations in Fig. 9 are illustrated for both τ commands in Fig. 13 and Fig. 14, showing both the control inputs and the τ signals.

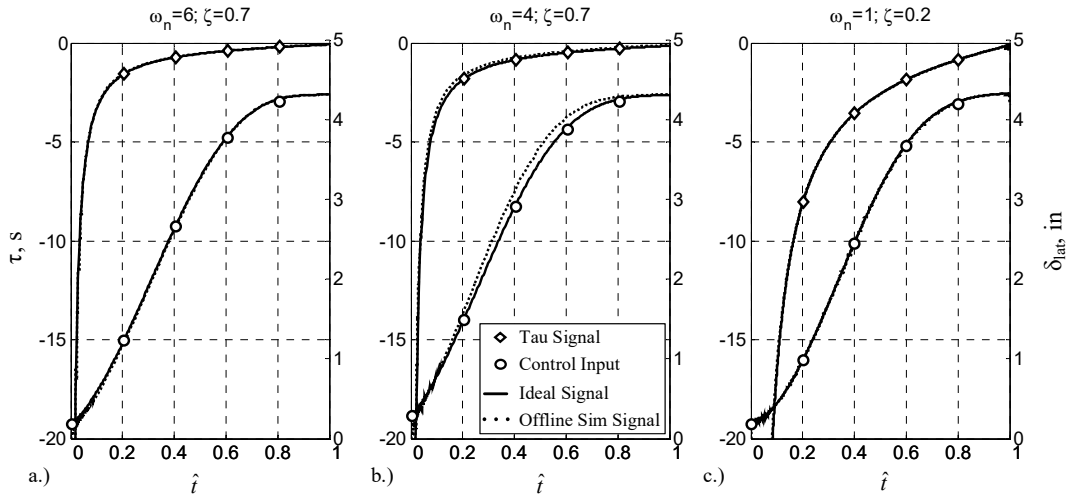

Fig. 13 Comparison between offline simulated and ideal pilot signals

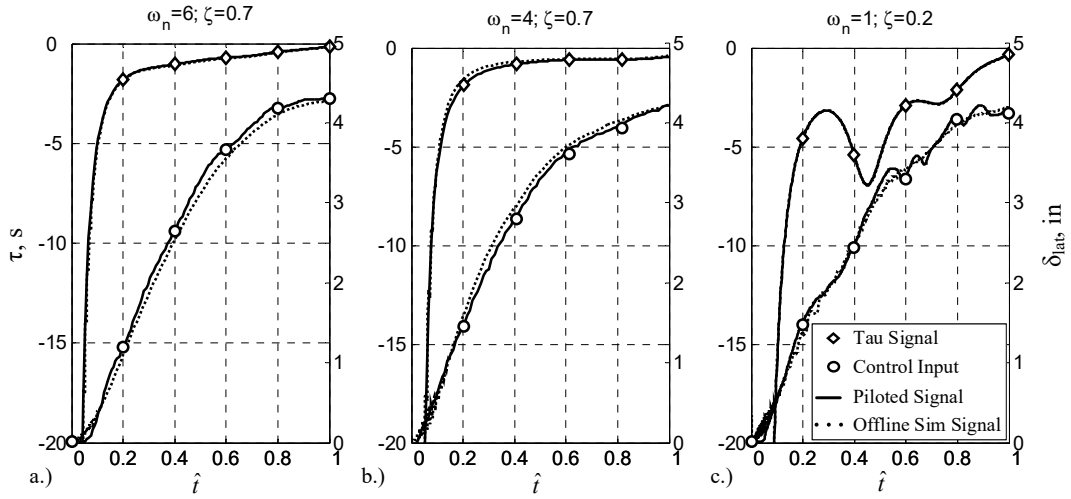

Fig. 14 Comparison between offline simulated and actual pilot signals

In Fig. 13, the Ideal τ using k and T values from Fig. 7 and Fig. 8 and the corresponding ideal control inputs from Eq. (13) are compared with the τ information (the feedback τ_x in Fig. 3) and the control input (after G_{nm}) from the offline simulation. In Fig. 14, the Piloted τ and actual pilot control inputs from the experiment are compared with the τ information (the feedback τ_x in Fig. 3) and the control input (after G_{nm}) from the offline simulation.

The results for both the control inputs and the τ signals of the postulated pilot-aircraft model derived using the two different τ-command signals show good agreement. Moreover, the difference between them (IFI < 4%) is much smaller than between the ideal (calculated) and actual pilot inputs shown in Fig. 9 (IFI < 15%). These results suggest that the pilot-aircraft model works effectively as a system inverter of the natural dynamics, even in the presence of

environmental noise (modelled in the visual quality model). This validates, to some extent, the controller structure adopted and its calculated gain values. The close fit indicates that the model, with the chosen K_P and K_L values in Fig. 12, is appropriate for simulating the lateral-reposition task.

The deviation between the actual and τ-guided ideal inputs, shown in Fig. 9, can now be revisited. The results of the offline simulation using the two sets of K_P and K_L values derived from the two τ-command signals in Fig. 12 reach a good fit, both with the Ideal τ and control inputs as shown in Fig. 13 and the actual piloted information shown in Fig. 14. The two sets of K_P and K_L values in Fig. 12 are therefore relevant to the actual input and τ-guided ideal input, respectively. The difference between the two sets of K_P and K_L values reflects the difference between the actual input and τ-guided ideal input shown in Fig. 9. As shown in Fig. 12, the corresponding lead terms K_L are almost the same. Therefore, the differences shown in Fig. 9 will generally be related to the K_P values of the ideal τ command that are generally larger than those obtained using the τ-command data from the actual pilot signal. In the regulator form of Eq. (9), the K_p term is, of course, the pilot gain. Larger predicted K_P values indicate that the pilot is using higher gains to achieve the ideal tracking signal, i.e. attempting to follow the τ-guide with a high precision. However, in practice, the pilot may choose a lower gain through increasing T, as suggested by the trend in Fig. 8. This allows the maintenance of a similar compensatory effort across the different aircraft dynamics that can be seen in Fig. 10. In turn, this reduces the fit between the actual pilot control input and τ-guided control input shown in Fig. 9.

Finally, the results in Fig. 13 and Fig. 14 again show that the natural dynamics of the system are suppressed in the overall dynamic response and the associated pilot inputs with both τ commands. For example, the oscillations in the actual pilot input shown in Fig. 14 are not present in the related input obtained from the offline simulation. This can be explained as follows. The command signal of the postulated pilot-aircraft model is generated from the guidance strategy following a CAG that depends only on the selected k and T values. Therefore, subject to properly selected K_P and K_L values, the response of the pilot-aircraft model in Fig. 3 will naturally follow the command signal, regardless of varying combinations of ω_n and ζ values. In other words, the inner dynamics of the controlled element are masked by the intrinsic closed-loop τ-guide process. This shows that the τ-guide model in Fig. 3, configured with appropriate K_P and K_L values, works effectively as an inverter, functioning as in Eq. (13). However, the model accomplishes the inversion in terms of a closed-loop feedback system whilst Eq. (13) is a simple and direct model inversion process.

VII. Discussion

The theoretical and experimental results presented in this paper provide support for the hypothesis that the test subjects adopted τ-guide control strategies to guide the ball to the target. The results in Fig. 7 indicate that the coupling term k is relatively insensitive to the variation of system (aircraft) dynamics. This finding is consistent with the previous research highlighted earlier in the paper. Unsurprisingly, the chosen maneuvering period T appears to be significantly affected by the dynamic system's natural frequency. As illustrated in Fig. 2, the shape of an ideal motion profile is uniquely determined by a given k value. The results therefore suggest that the pilot adapts T to the aircraft's dynamics, to achieve the desired performance, a skill developed perhaps through developed through initial training and reinforced through recurrent trainings. Moreover, this adaptation of T reveals how a pilot can maintain similar compensatory effort (Fig. 10) by varying workload across a range of dynamic systems (Fig. 11).

A linearization procedure has been used to model τ-perception as a lead process, which is reasonable in that τ theory posits that motion perception and control needs to be prospective, with some degrees of extrapolation into the future [14]. A question that arises from the pilot-aircraft model shown in Fig. 3, is which pathway does the τ-guide function reside at the perceptual level? The classic structure includes three perceptual pathways for pilot control activities: compensatory, pursuit, and precognitive [6]. Within this structure, the τ-guide is analogous to the definition given by McRuer et al. for precognitive pilot control [7]:

"The operator with the precognitive control can generate neuromuscular commands, which are deft, discrete, properly timed, scaled, and sequenced so as to result in machine outputs which are exactly as ideal. The neuromuscular commands are selected from a repertoire of previously learned control movements."

As a directly perceived optical variable, τ, and the associated τ guidance, are therefore modelled as a kind of precognitive control, whereby the combination of the τ of the motion gap and the internal motion guide generate neuromuscular commands that result in the controlled element closing the ideal motion gaps [7]. Through practice and training, it may be that the pilot tends to use "preferred" k values (Fig. 7). This has been found in the above analyses as well as in [3;15;18]. These "preferred" values form the ideal tracking signal (τ_g) and then guide the motion of the controlled element using τ coupling. This type of high-level τ-guide control therefore appears to be open-loop, but essentially works in a closed-loop form in concert with the regulating operation introduced in Fig. 3. Therefore, the pilot-aircraft model structure proposed in Fig. 3 is actually a dual-model control structure, where the precognitive

action initiates the control and guides the tracking process, and is augmented by a regulating process to reduce the tracking error.

Previous research has shown that τ-guided flight appears to suppress the natural aircraft dynamics. The analysis presented in this paper shows that an important aspect of τ guidance is a system inversion process, generating appropriate pilot control inputs by regulating the available information from the optical field to follow the required trajectory, using the pilot's selected k and T values. The suppression of the internal dynamics in Eq. (13) means that the open-loop poles in the aircraft dynamic system will not play a role in determining the dynamics of the closed-loop system. If this is interpreted within the closed-loop structure of the dual model in Fig. 3, the internal aircraft dynamics are effectively masked by the regulating closed loops.

VIII. Conclusions and Future Work

This paper has investigated pilot guidance adaptation to varying system dynamics with the aim of developing a pilot-aircraft model to describe motion control using time-to-contact (τ). The pilot-aircraft model proposed is modelled as a closed-loop feedback system, where, for the first time, the loop is closed using directly perceived τ information. A CAG is assumed to activate the guidance with the pilot adjusting the τ coupling k and maneuver time T. The experiments and analyses conducted and the model developed allow the following conclusions to be drawn. Firstly, it appears that pilots adopt a similar coupling constant, k, whilst adjusting the maneuver period, T, for varying system dynamics. Secondly, this paper provides a linearization process for sensing τ information that delivers excellent results in terms of matching pilot-aircraft model output and experimental results. Thirdly, the pilot-aircraft model proposed explains the apparent open-loop nature of τ guidance by showing that the pilot closes a feedback loop for stabilization and guidance functions as a regulator plus inverter; the τ-guidance strategy is behaving as the inverter of the aircraft dynamics, allowing the ideal/desired motion trajectory to be followed. Finally, based on the hypothesis that the τ-guide is a learned response, a mental model for closing the desired motion gap, and within the hierarchical framework of perception, the results suggest that τ-guidance functions at a precognitive level.

Whilst the proving or otherwise of τ theory as a perceptual mechanism is beyond the scope of this work, the success of a theory lies in its general explanatory power and the degree to which it is supported by empirical evidence. The data, analyses and results in this paper do indeed provide further evidence that τ theory is a useful mechanism for modelling piloting guidance strategies. It is planned to extend the current investigation of the pilot-aircraft model to

unstable or non-minimum phase problems and to maneuvering tasks where the time to complete the task is constrained. Our research will also include investigations into the simultaneous closure of multiple gaps of which there are many examples in flight control.

Acknowledgments

The research leading to these results was partly supported by funding from the European Community's Seventh Framework Programme (ARISTOTEL FP7/2007-2013) under grant agreement N° 266073.

Appendix

A. Determination of Regulator Parameters

Table A1 Derivations of motion forms for constant acceleration guide

$v_g = v_{g0} + a_{g0}\, t,\ a_g = a_{g0}$		$\hat{x} = -(1-\hat{t}^2)^{1/k}$
$x_g = x_{g0} + v_{g0}\, t + \frac{a_{g0}}{2} t^2, v_{g0} = 0$		$\dot{\hat{x}} = \frac{2\hat{t}}{k}(1-\hat{t}^2)^{(\frac{1}{k}-1)}$
$x_g = x_{g0}(1-\hat{t}^2)$		$\ddot{\hat{x}} = -\frac{2}{k}\left(\left(\frac{2}{k}-1\right)\hat{t}^2 - 1\right)(1-\hat{t}^2)^{(\frac{1}{k}-2)}$
$v_g = -\frac{2x_{g0}}{T}\,\hat{t}$		
$a_g = a_{g0} = -\frac{2x_{g0}}{T^2}$	$\tau_x = k\,\tau_g, x = C\, x_g^{\,1/k}$	$\hat{\tau}_{\hat{x}} = \frac{k}{2}\left(\hat{t} - \left(\frac{1}{\hat{t}}\right)\right)$
$\tau_g = -\frac{T}{2}(\frac{1}{\hat{t}} - \hat{t})$		$\dot{\hat{\tau}}_{\hat{x}} = \frac{k}{2}\left(1 + \left(\frac{1}{\hat{t}}\right)^2\right)$
$\hat{\tau}_g = -\frac{1}{2}(\frac{1}{\hat{t}} - \hat{t})$		$\dot{\hat{x}}(0) = \frac{2}{k}$
$\tau_g' = \dot{\hat{\tau}}_g = \frac{1}{2}(1+\frac{1}{\hat{t}^2})$		$T = -\sqrt{\frac{2x(0)}{k\,\ddot{x}(0)}}$

Table A2 Aircraft kinematics with different *k* values; following an intrinsic *τ* guidance

No.	*k*	Aircraft Motion
1	$k > 1.0$	Increasing acceleration towards the goal/boundary
2	$k = 1.0$	Constant acceleration towards the goal/boundary
3	$0.5 < k < 1.0$	Acceleration-Deceleration, maximum velocity late in maneuver, stopping at the boundary with residual speed (hard stop)
4	$k = 0.5$	Acceleration-Deceleration, stopping just at the boundary
5	$0 < k < 0.5$	Acceleration-Deceleration, maximum velocity early in maneuver, stopping at the boundary with zero residual speed (soft stop)

References

[1] Padfield, G. D., *Helicopter Flight Dynamics,* 2nd ed., Blackwell Science, Oxford, 2007, pp. 517-559. Doi: 10.1002/9780470691847.ch8.

[2] Padfield, G. D., Charlton, M. T., Jones, J. P., Howell, S. E., and Bradley, R., "Where Does the Workload Go When Pilots Attack Maneuvers? An Analysis of Results from Flying Qualities Theory and Experiment," *20th European Rotorcraft Forum*, Paper 83, Amsterdam, Oct.4th -7th 1994.

[3] Padfield, G. D., "The Tau of Flight Control," *Aeronautical J*, Vol. 115, No. 1171, Sept. 2011, pp. 521–555.

[4] McRuer, D. T., and Jex, H. R., "A Review of Quasi-Linear Pilot Models," *IEEE Transactions on Human Factors in Electronics*, Vol. 8, No. 3, Sept. 1967, pp. 231-249. Doi: 10.1109/THFE.1967.234304.

[5] McRuer, D. T., and Krendel, E. S., "Mathematical Models of Human Pilot Behavior," AGARD-AG-188, Jan.1974.

[6] McRuer, D. T., Clement, W. F., Thompson, and Magdaleno., R. E., "Minimum Flying Qualities Volume II: Pilot Modelling for Flying Qualities Application," Flight Dynamics Laboratory, Air Force Systems Command, Wright-Patterson Air force Base, OHIO, WRDC-TR-89-3125, Jan.1990.

[7] McRuer, D. T., "Pilot-Induced Oscillations and Human Dynamic Behavior," NASA Contractor Report 4683, Jul.1995.

[8] Bradley, R., and Thomson, D. G., "Inverse Simulation as A Tool for Flight Dynamics Research - Principles and Applications," *Aeronautical J*, Vol. 42, No. 3, May.2006. pp. 174-210. Doi: 10.1016/j.paerosci. 2006.07.002.

[9] Lu, L., Murray-Smith, D. J., and Thomson, D. G., "Sensitivity-Analysis Method for Inverse Simulation Application", J Guid Contr Dynam, Vol. 30, No. 1, Jan.2007, pp. 114-121. Doi: 10.2514/1.20722.

[10] Snell, S. A., Enns, D. F., and Jr. Garrard, W. L., "Nonlinear Inversion Flight Control for A Super Maneuverable Aircraft," *J Guid Contr Dynam*, Vol. 15, No. 3, Jul.1992, pp. 976-983. Doi: 10.2514/3.20932.

[11] Lu, W. C., El-Moudani, W., Revoredo, T. C., and Mora-Camino, F., "Neural Networks Modelling for Aircraft Flight Guidance Dynamics," *J. Aerosp. Technol. Manag.*, Vol. 4, No. 2, Apr.2012, pp. 169-174. Doi: 10.5028/jatm.v4i2.152.

[12] Lee, D. N., "Guiding Movement by Coupling Taus," *Ecological Psychology*, Vol. 10, No. 3, 1998, pp. 221-250. Doi:10.1207/s15326969eco103&4_4.

[13] Keil, M. S., and López-Moliner, J., "Unifying Time to Contact Estimation and Collision Avoidance Across Species," *PLoS Comput Biol*, Vol. 8, No. 8, Aug.2012, pp. 1-13. Doi: 10.1371/journal.pcbi.1002625.

[14] Lee, D. N., Craig, C. M., and Grealy, M. A., "Sensory and Intrinsic Coordination of Movement," *Proc. of Biological sciences*, Vol. 266, No. 1432, Jul. 1999; pp. 2029-2035. Doi: 10.1098/rspb.1999.0882.

[15] Lee, D. N., "Tau in Action in Development," *Action as an Organizer of Learning and Development*, edited by. J. J. Rieser, J. J. Lockman, and C. A. Nelson, 33rd Vol in the Minnesota Symposium on Child Psychology, Minnesota, 2005, pp. 3-50.

[16] Padfield, G. D., Lee, D. N., and Bradley, R., "How Do Helicopter Pilots Know When to Stop, Turn or Pull Up?," *Journal of the AHS*, Vol. 48, No. 2, 2003, pp. 108-119. Doi: 10.4050/JAHS.48.108.

[17] Padfield, G. D., Clark, G., and Taghizad, A., "How Long Do Pilots Look Forward? Prospective Visual Guidance in Terrain-Hugging Flight," *Journal of the AHS*, Vol. 52, No. 2, 2007, pp. 134-145.

[18] Jump, M., and Padfield, G. D., "Investigation of the Flare Maneuver Using Optical Tau," *J Guid Contr Dynam*, Vol. 29, No. 5, Sept. 2006, pp. 1189-1200. Doi: 10.2514/1.20012.

[19] Jump, M., and Padfield, G. D., "Progress in the Development of Guidance Strategies for the Landing Flare Maneuver Using Tau-based Parameters," *Aircraft Eng Aero Tech*, Vol. 78, No. 1, 2006, pp. 4-12. Doi: 10.1108/17488840610639618.

[20]. Clark, G., "Helicopter Handling Qualities in Degraded Visual Environments," PhD Thesis, Department of Engineering, The University of Liverpool, UK, 2007.

[21] Padfield G.D., Lu, L., and Jump, M., "Tau Guidance in Boundary-Avoidance Tracking - New Perspectives on Pilot-Induced Oscillations," *J Guid Contr Dynam*, Vol. 35, No. 1, 2012, pp. 80-92. Doi: 10.2514/1.54065.

[22] Tresilian, J.R., "Four Questions of Time to Contact: A Critical Examination of Research On Interceptive Timing," *Perception*, 2003; Vol 22, pp. 653-680. Doi: 10.1068/p220653.

[23] White, M. D., Padfield, G. D., Armstrong, R., "Progress with the Adaptive Pilot Model in Simulation Fidelity", *50th Annual Forum of the American Helicopter Society*, Baltimore, MD, June 2004.

[24] Anon., "*Handling Qualities Requirements for Military Rotorcraft US Army Aviation and Missile Command*," ADS-33E-PRF, 2000.

[25] Voskuijl, M., Padfield, G. D, Walker, D. W, Manimala, B., and Gubbels, A. W., "Simulation of Automatic Helicopter Deck Landings Using Nature Inspired Flight Control," *Aeronautical J*, Vol 114, No 1151, Jan.2010, pp. 25-34.

[26] Izzo, D., Weiss, N., and Seidl, T., "Constant-Optic-Flow Lunar Landing: Optimality and Guidance," *J Guid Contr Dynam*, Vol. 34, No. 5, Sept. 2011, pp. 1383-1395. Doi: 10.2514/1.52553.

[27] Franceschini, N., Ruffier, F., Serres, J., and Viollet, S., "*Optic Flow Based Visual Guidance: From Flying Insects to Miniature Aerial Vehicles,*" edited by. Lam, T. M. in Aerial Vehicles, 2009, pp. 747-770.

[28] Delafield-Butt, J., Galler, A., Schögler, B., and Lee, D. N., "A Perception - Action Strategy for Hummingbirds", *Perception*, Vol, 39, No, 9, 2010, pp. 1172-1174. Doi: 10.1068/p6708.

[29] Kendoul, F., and Ahmed, B., "Bio-inspired Taupilot for Automated Aerial 4D Docking and Landing of Unmanned Aircraft Systems," *2012 IEEE/RSJ International Conference on Intelligent Robots and Systems, IROS 2012*, Vilamoura, Algarve, Portugal, Oct. 7th-12th, 2012, pp.480-487.

[30] de Croon, G. C. H. E., Izzo, D., and Schiavone, G., "Time-to-Contact Estimation in Landing Scenarios Using Feature Scales," *ACTA FUTURA*, Vol 5, Jan. 2012, pp. 73-82.

[31] Hess, R. A., “Simplified Approach for Modelling Pilot Pursuit Control Behaviour in Multi-Loop Flight Control Tasks,” *Proceedings of the I MECH E Part G Journal of Aerospace Engineering*, published online 2006; Vol. 220, No. 2, pp. 85-102. Doi: 10.1243/09544100JAERO33.

[32] Bootsma, R. J., and Craig, C. M., "Information Used in Detecting Upcoming Collision,” *Perception*, Vol. 32, No. 5, 2003, pp. 525-544. Doi: 10.1068/p3433.

[33] Isidori, A. *Nonlinear Control Systems,* 3rd ed., Springer Verlag, London, 1995.

[34] Hess, R.A., “Obtaining Multi-Loop Pursuit-Control Pilot Models from Computer Simulation,” *Proc. of the I MECH E Part G Journal of Aerospace Engineering*, Vol. 222, No. 2, Feb. 2008, pp. 189-199. Doi: 10.1243/09544100JAERO260.

[35] Yilmaz, D., Pavel, M. D., Jones, M., Jump, M., and Lu, L., “Identification of Pilot Control Behavior during Possible Rotorcraft Pilot Coupling Events”, *38th European Rotorcraft Forum*, Amsterdam, the Netherlands, 4th - 7th Sept, 2012.

[36] Hess, R.A., and Siwakosit, W., “Assessment of Flight Simulator Fidelity in Multiaxis Tasks Including Visual Cue Quality,” *Journal of Aircraft*, published online Jul. 2007; Vol. 38, No. 4, pp. 607-614. doi: 10.2514/2.2836.

[37] White, M., Perfect, P., Padfield, G. D., "Acceptance Testing and Commissioning of A Flight Simulator for Rotorcraft Simulation Fidelity Research," *Proc, of the Institution of Mechanical Engineers*, *Part G: Journal of Aerospace Engineering*, Vol. 227, No. 4, 2012, pp. 663-686. Doi: 10.1177/0954410012439816.

[38] Padfield, G. D., and White, M. D., “Flight Simulation in Academia; HELIFLIGHT in Its First Year of Operation,” *Aeronautical Journal*, published online Sept. 2003; Vol. 107, No. 1075, pp. 529-538.

[39] Anonymous, MIL-HDBK-1797 Flying Qualities of Piloted Aircraft, Department of Defense Interface Standard, 1990.

[40] Lu, L., Murray-Smith, D. J., and McGookin, E. W., “Investigation of inverse simulation for design of feedforward controllers”, *Mathematical and Computer Modeling of Dynamical Systems: Methods, Tools and Applications in Engineering and Related Sciences*, Vol. 13, No. 5, 2007, pp. 437-454. Doi: 10.1080/ 13873950701344023.

[41] Golnaraghi, F., and Kuo, B., *Automatic Control Systems*, Wiley-Blackwell, NJ Wiley, 2003.